

Article

A New Function of *MbIAA19* Identified to Modulate *Malus* Plants Dwarfing Growth

Jian Wang, Li Xue, Xiao Zhang , Yali Hou, Ke Zheng, Dongxu Fu and Wenxuan Dong *

College of Horticulture, Shenyang Agricultural University, Shenyang 110866, China; botelongma@163.com (J.W.); lixue@syou.edu.cn (L.X.); zhangxiao8866@syou.edu.cn (X.Z.); houyali@syou.edu.cn (Y.H.); zhengke19870430@163.com (K.Z.); f18547590930@163.com (D.F.)

* Correspondence: dongwx63@syou.edu.cn

Abstract: The primary determinants of apple (*Malus*) tree architecture include plant height and internode length, which are the significant criteria for evaluating apple dwarf rootstocks. Plant height and internode length are predominantly governed by phytohormones. In this study, we aimed to assess the mechanisms underlying dwarfism in a mutant of *Malus baccata*. *M. baccata* dwarf mutant (*Dwf*) was previously obtained through natural mutation. It has considerably reduced plant height and internode length. A comparative transcriptome analysis of wild-type (WT) and *Dwf* mutant was performed to identify and annotate the differentially expressed genes responsible for the *Dwf* phenotype using RNA-seq and GO and KEGG pathway enrichment analyses. Multiple DEGs involved in hormone signaling pathways, particularly auxin signaling pathways, were identified. Moreover, the levels of endogenous indole-3-acetic acid (IAA) were lower in *Dwf* mutant than in WT. The Aux/IAA transcription factor gene *MbIAA19* was downregulated in *Dwf* mutant due to a single nucleotide sequence change in its promoter. Genetic transformation assay demonstrated strong association between *MbIAA19* and the dwarf phenotype. *RNAi-IAA19* lines clearly exhibited reduced plant height, internode length, and endogenous IAA levels. Our study revealed that *MbIAA19* plays a role in the regulation of dwarfism and endogenous IAA levels in *M. baccata*.

Keywords: Aux/IAA; auxin; dwarf; *Malus baccata*; transcriptome



Citation: Wang, J.; Xue, L.; Zhang, X.; Hou, Y.; Zheng, K.; Fu, D.; Dong, W. A New Function of *MbIAA19* Identified to Modulate *Malus* Plants Dwarfing Growth. *Plants* **2023**, *12*, 3097. <https://doi.org/10.3390/plants12173097>

Academic Editor: Nobutoshi Yamaguchi

Received: 11 July 2023

Revised: 5 August 2023

Accepted: 21 August 2023

Published: 29 August 2023



Copyright: © 2023 by the authors. Licensee MDPI, Basel, Switzerland. This article is an open access article distributed under the terms and conditions of the Creative Commons Attribution (CC BY) license (<https://creativecommons.org/licenses/by/4.0/>).

1. Introduction

Dwarfing and tightly separated planting are the primary modes of modern fruit farming practices. Over the past century, extensive application of dwarfing rootstocks has led to increased planting density and production of fruits, even during early years of orchard development [1,2]. The complex features of plant dwarfism are regulated by multiple genes, such as *PcPIN1*, *OsBR6ox*, *PsGA3ox1*, *WRKY*, and *GRAS* [3–7]. Multiple mutants with dwarfing associated with phytohormones were uncovered, such as rice, maize, and apple, and the underlying gene functions were confirmed [8–10]. Phytohormones act as central players in the regulation of plant growth and development, in which auxin is the most significant signaling molecule because it is involved in almost all aspects of plant life. The development and phenotype of several organs could be influenced by auxin, including the root system, plant height, leaf shape, and reproductive organs, resulting in cell division and cell expansion at various stages of tissue development [11–14]. Clarifying the association between auxin and plant phenotypes is essential for understanding the mechanism of dwarfism in plants.

Auxins modify the expression of downstream genes that encode proteins involved in a wide range of physiological networks in plants [15–17]. Extensive studies have reported that auxins regulate the expression of downstream genes through ubiquitin-dependent proteolytic signal transduction system. First, transport inhibitor response1 (TIR1) protein forms a multi-subunit SCF ubiquitin ligase. Further, the complex interacts with auxin/indole-3-acetic acid (Aux/IAA), which is a transcriptional repressor that inhibits the expression of

early auxin-responsive genes, eventually leading to the degradation of Aux/IAA proteins by the proteasome [18]. The affinity of TIR1 for Aux/IAA is influenced by the concentration of cellular auxin. High concentration of auxin induces the degradation of Aux/IAA; however, low concentration of auxin reduces the interaction between TIR1 and Aux/IAA [19]. Aux/IAA inhibits the transcriptional activity of auxin responsive factors (ARFs), which regulate the expression of genes that respond to auxin, by directly interacting with them. Thus, Aux/IAs are crucial for controlling auxin-mediated activities [20,21].

Aux/IAA repressor proteins contain four highly conserved domains (I–IV). Of these, domain II, also known as the degron motif, is primarily responsible for the auxin-dependent degradation of Aux/IAs [22]. Gain-of-function mutations in domain II of the Aux/IAA in *Arabidopsis thaliana* provided information on the role played by these proteins in modulating auxin responses and plant developmental processes. These mutations may reduce or abolish the interactions among TIR1 and Aux/IAs. Many auxin-related developmental abnormalities, such as altered lateral root formation, stem hypocotyl elongation, leaf expansion, apical dominance, phototropism, and gravitropism, are displayed by these Aux/IAA gain-of-function mutants [23–27]. Genetic studies have revealed various morphological phenotypes in association with Aux/IAA genes in other plant species. Fewer crown and lateral roots were produced in rice (*Oryza sativa*) due to the negative regulation of auxin-regulated root development by *Osiaa9* [28]. Tomato (*Solanum lycopersicum*) plants with *SlIAA15* silencing exhibited reduced apical dominance and number of trichomes; thick, dark-green leaves with thicker pavement cells; longer palisade cells; and spongy mesophyll cells that have a wider intercellular space [29]. Plants with *SlIAA9* silencing exhibited abnormally shaped leaves, enhanced stem elongation, and increased leaf vascularization [30]. *Brassica napus* IAA7 gain-of-function mutant inhibited stem elongation due to the transcriptional repression of *EXPA5* genes [31]. The overexpression of *PtoIAA9m* in *Populus* significantly repressed the development of secondary xylem [32]. When *TaIAA15* was ectopically expressed in rice, plant height and leaf angle were reduced [33]. In apple, *MdIAA2* overexpression led to the formation of smaller fruit [34]. The overexpression of *PpIAA19* (from peach (*Prunus persica*)) in tomato altered the plant development and fruit shape and substantially lengthened the internodes [35]. *OsIAA23*-knockout genotypes in rice exhibited significantly higher dwarfing and abnormalities in lateral root development [36]. Aux/IAA genes are extensively involved in determining plant height and regulating many other phenotypes. They can act as promoters or suppressors.

Apple (*Malus domestica*) is one of the most important commercial fruits. Generating dwarfing rootstocks and apple cultivars is important for improving economic yield and efficient orchard management. NIAB East Malling Research Station, England, conducts breeding to obtain dwarf rootstocks; after a century of development, many locally adapted dwarf rootstocks of apple were generated, such as M9, M26, and GC lines [37,38]. In northern China, *M. baccata* is frequently used as an apple rootstock because of its strong tolerance to cold and drought stresses. In this study, we aimed to assess the mechanisms underlying dwarfing in apple. We characterized an *M. baccata* dwarf mutant (*Dwf*), which exhibits shorter stature and internode lengths than the wild type (WT). RNA-seq, metabolites analysis, and extensive biological experiments were performed to reveal a novel function of *MbIAA19* associated with the phenotype of *Dwf*. This study provided a foundation for clarifying the relationship among *MbIAA19*, auxin, and dwarfism. Understanding the mechanism of dwarfism in *Dwf* will help in breeding rootstocks with better adaptability to various stresses.

2. Results

2.1. *Dwf* Mutant Exhibited Variation in the Phenotype of Multiple Organs

The plant height and internode length are important indicators of dwarfism. The spontaneous dwarf mutant of *M. baccata*, namely, the *Dwf* mutant, exhibited shorter plant height and internodes and lower leaf index than WT (Figure 1A–C). Observations revealed that compared with WT, *Dwf* mutant exhibited 1.6-fold shorter plant height, and its internode

length, leaf index, and leaf length were reduced by 30% (Figure 1D,E), 34% (Figure 1F), and 38% on an average, respectively (Figure 1G). However, no discernible variation in leaf breadth was observed (Figure 1H). Surprisingly, *Dwf* mutant represents distinct curled leaves (Figure 1C).

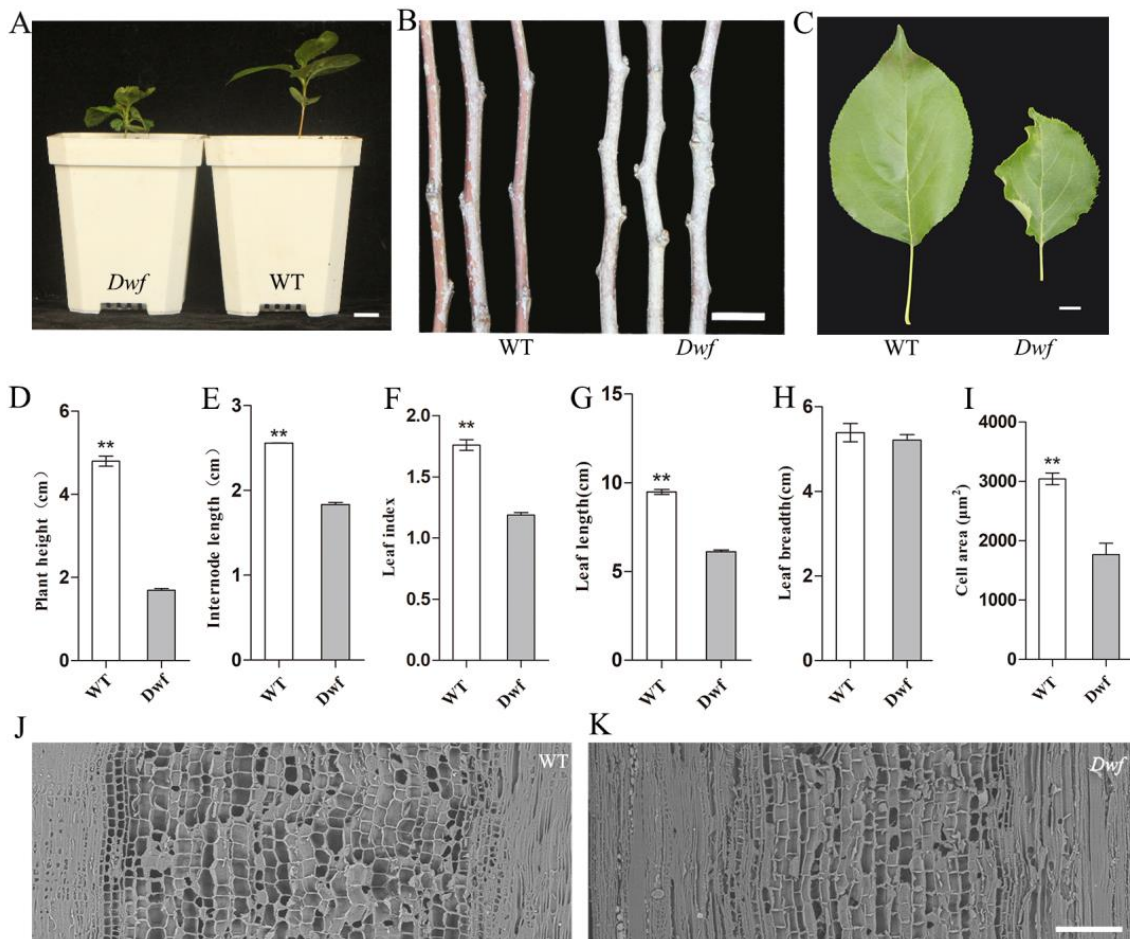


Figure 1. Morphological characterization of *Dwf* mutant. (A) Universal morphology of the dwarf mutant (*Dwf*) and wild type (WT) plants of *M. baccata* after 1 month of culture. Scale bar = 1 cm. (B) Annual branches of WT and *Dwf* plants. Scale bar = 1 cm. (C) Apical leaves of the annual branches of WT and *Dwf* plants. Scale bar = 1 cm. (D) Plant heights of WT and *Dwf* plants. (E) Internode lengths of the annual branches of WT and *Dwf* plants. (F) Calculation of the leaf length to width ratio of the WT and *Dwf* plants. (G) Leaf length of WT and *Dwf* plants. (H) Leaf breadth of WT and *Dwf* plants. (I) Cell areas of stem vessels in longitudinal sections. (J,K) Scanning electron microscopic observation of the longitudinal section of stems in annual branches of WT and *Dwf* plants. Scale bar = 0.2 mm. The asterisks above the error bars in (D–G,I) indicate significant differences at $p < 0.01$ using a one-way analysis of variance (ANOVA) and Dunnett's test.

The cytological differences in the two genotypes were studied using SEM. The cell area in the xylem regions of annual branches of the *Dwf* was 42% smaller than the WT (Figure 1I); it revealed that there were dramatically smaller longitudinal vascular bundles cells in the annual branches of the *Dwf* mutant than in the WT (Figure 1J,K).

Furthermore, the root morphology, flowers, and fruits of *Dwf* mutant were significantly altered. It exhibited shorter primary roots (PR) (Figure 2A,B), fewer lateral roots (LR) (Figure 2C,D), and decreased corolla width and fruit diameter (Figure 2E–H).

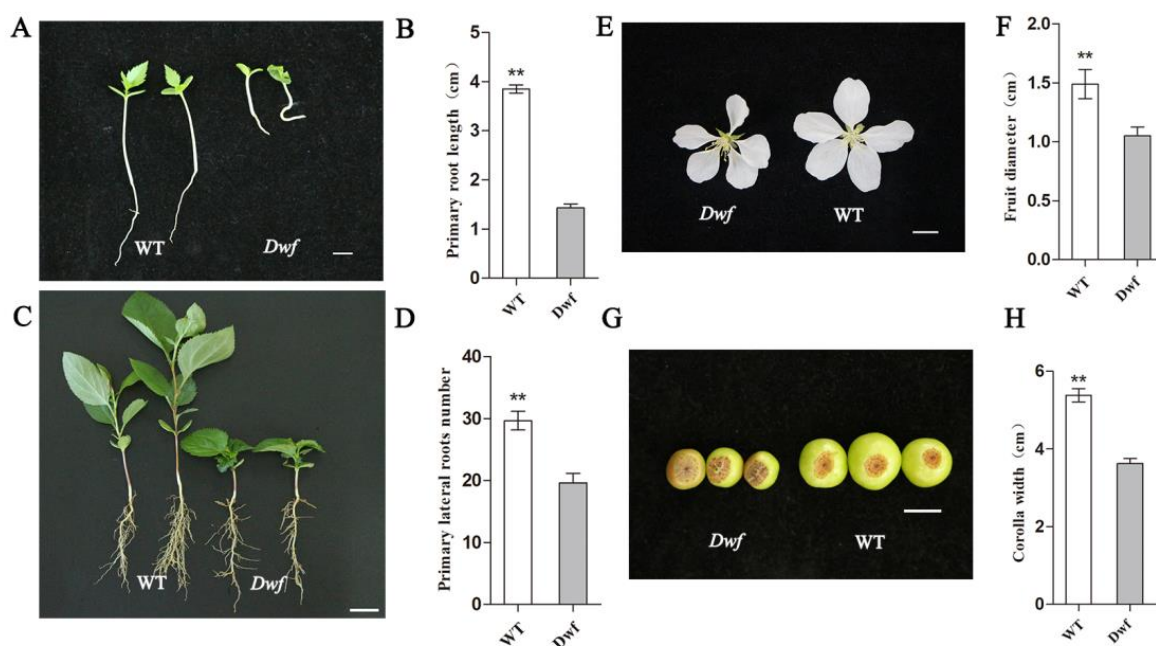


Figure 2. Morphological characterization of the root, flower, and fruit of the *Dwf* mutant. (A) Primary roots of one-week-old WT and *Dwf* plants. (B) Length of primary roots. (C) Lateral roots of WT and *Dwf* plants after 1 month of culture. (D) Quantitative analysis of primary lateral root number. (E) Flowers, (F) corolla width, (G) fruits, and (H) fruit diameter of WT and *Dwf* mutant. The asterisks above the error bars in (B,D,F,H) indicate significant differences at $p < 0.01$ using a one-way analysis of variance (ANOVA) and Dunnett's test. Scale bar = 1 cm.

2.2. Analysis of the DEGs on Phytohormone RNA-seq Data

To further understand the regulatory mechanism of dwarfism in *Dwf* plants, RNA-seq was performed to study the transcription profiles and identify the DEGs responsible for the *Dwf* phenotype. Young leaves at the tips of annual branches were collected from six individual plants (WT 1–3 and *Dwf* 1–3) for RNA-seq analysis. GO and KEGG pathway enrichment analysis revealed numerous genes associated with signal transduction via phytohormones and hormone response processes (Figure S1A,B). Compared with WT, 352 and 460 genes were up- and downregulated, respectively, in the *Dwf* plants ($\log_2 \geq 1$) (Figure S1C). A total of 17 hormone-signaling- and growth-related genes were subjected to qRT-PCR to verify the DEGs (Figure S2A,B). The results of RNA-seq and qRT-PCR were consistent.

To thoroughly investigate the complete transcriptional pattern of DEGs related to phytohormones, DEGs associated with the signaling and biosynthetic pathways of IAA, ethylene (ET), jasmonic acid (JA), GA, brassinosteroids (BR), cytokinin (CK), and abscisic acid (ABA) were further functionally annotated. Crucial proteins involved in the auxin signal transduction pathway were altered. The auxin-responsive genes, including *MbAUX/IAA19* and *MbSAURs*, were overall downregulated (Figure 3A). *MbAUX/IAA19* is one of the major molecular components involved in auxin signaling, and *SAURs* regulate the cell expansion which has been demonstrated [39]. In addition, auxin efflux carrier components (*MbPIN1* and *MbPIN6*) were significantly downregulated in *Dwf* mutant (Figure 3A). DEGs associated with ET signaling such as *EIN3*-binding *F-box* genes (*MbEBF1s*), which physically interact with *EIN3* and *EIL1* proteins for degradation, were upregulated in *Dwf* mutant [40]. ET-biosynthesis-related genes (*MbACO4*, *MbACS6*, and *MbACS10*) were upregulated, whereas three ET-responsive transcription factors genes (*MbERF1A*, *MbERF1B*, and *MbERF060*) were downregulated in *Dwf* (Figure 3B). *MbTYFYs* (JAZs) involved in the JA signaling pathway were downregulated in *Dwf* mutant, the depletion of JAZ proteins

is also associated with reduced growth and development [41]; MYC2, a key transcription factor (TF) of JA signaling pathway, was downregulated in *Dwf* mutant (Figure 3C).

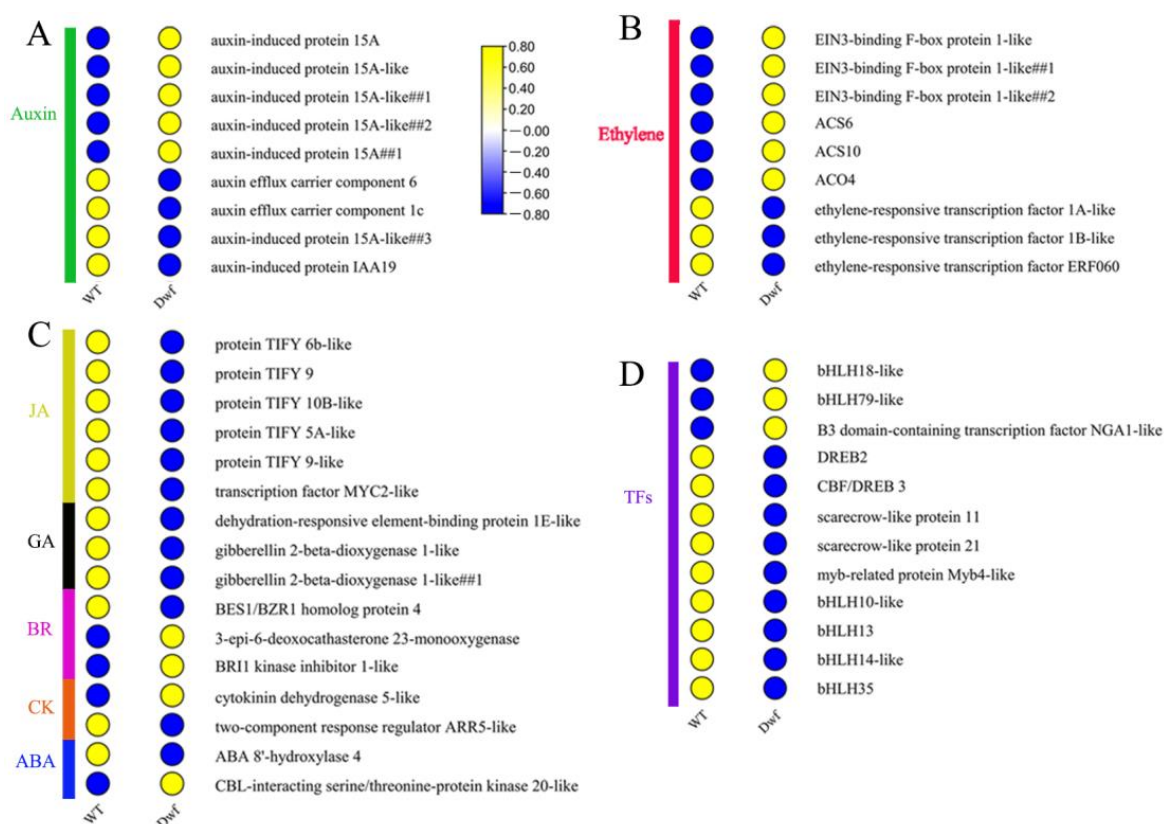


Figure 3. A heatmap of differentially expressed genes (DEGs) associated with phytohormone pathways. (A) DEGs associated with the signaling and biosynthesis pathways of auxin. (B) DEGs associated with the signaling and biosynthesis pathways of ethylene. (C) DEGs related to the signaling and biosynthesis pathways of JA, GA, BR, CK, and ABA. (D) Transcription factors involved in hormone signaling.

GA, BR, CK, and ABA signaling pathways were altered in *Dwf* (Figure 3C). Among GA signaling genes, *MbDREB1E* (dehydration-responsive element-binding protein 1E) and *MbGA20OX1* (gibberellin 2-beta-dioxygenase 1; responsible for the bioactive transformation of GAs) were downregulated. Additionally, several genes related to signaling and biosynthesis of BR, CK, and ABA were altered. *BRI1-EMS-SUPPRESSOR1/BRASSINAZOLE RESISTANT4* (*BES1/BZR4*) plays a key role in BR signaling, was downregulated in *Dwf*. Similarly, *BKI1* act as a negative regulator of BR signalling and was up-regulated in *Dwf* (Figure 3C). Cytokinin oxidase/dehydrogenase5 (*CKX5*), a destructor of cytokinin, was up regulated in *Dwf* (Figure 3C). ABA 8'-hydroxylation act as the major components involved in catabolic pathway of ABA and was downregulated in *Dwf* (Figure 3C). TFs involved in hormone signaling were downregulated in *Dwf* plants (Figure 3D). These results demonstrate that the phytohormone signaling and biosynthetic pathways were affected in the *Dwf* mutant. Interestingly, 26% DEGs involved in phytohormone signaling were associated with the auxin signaling pathway. Therefore, auxin was observed to be an essential hormone in controlling plant growth in *Dwf* mutants.

2.3. Endogenous Auxin Levels Were Lower in *Dwf* Mutant

To investigate whether DEGs related to auxin signaling and biosynthesis pathways are associated with the change in endogenous auxin levels, endogenous IAA levels were detected in both genotypes. Endogenous IAA content was substantially lower in the leaves

of the *Dwf* mutant than in those of the WT (Figure 4A). We investigated whether auxin deficiency in *Dwf* mutant affected the dwarfing. One-month-old *Dwf* seedlings were sprayed with $0.4 \text{ mg}\cdot\text{L}^{-1}$ IAA once a week for 4 weeks and plant growth was observed. Interestingly, plant height was significantly increased in the *Dwf* mutant after IAA treatment compared to after water treatment (Figure 4B,C). These findings suggested that the endogenous auxin levels were altered in the *Dwf* mutant, and this alteration played a key role in dwarfing.



Figure 4. Analysis of endogenous auxin levels and exogenous auxin treatment. (A) Endogenous auxin levels in WT and *Dwf* mutant leaves. (B) *Dwf* mutant plants were sprayed with $2.3 \mu\text{M}$ IAA once a week for 4 weeks. Growth status of *Dwf* mutant before and after auxin treatment. (C) Plant height increased after treatment with $0.4 \text{ mg}\cdot\text{L}^{-1}$ IAA than after that with water for 1 month. The asterisks above the error bars indicate significant differences at $p < 0.01$ calculated using a one-way analysis of variance (ANOVA) and Dunnett's test.

2.4. Analysis of *MbIAA19* Gene Expression and Promoter Sequence

MbIAA19 is a member of the AUX/IAA gene family. Sequence analysis revealed that *MbIAA19* contains an open reading frame of 573 bp, encoding 190 amino acids; the *MbIAA19* sequences from WT and *Dwf* were identical. After aligning with IAA19 protein sequences from *P. persica* and *A. thaliana*, it was revealed that *MbIAA19* proteins contain four conserved domains (domains I, II, III, and IV; Figure 5A). The expression of *MbIAA19* in several tissues was studied using qRT-PCR. It was significantly downregulated in the roots, stems, and leaves of *Dwf* plants (Figure 5B). Next, we performed a subcellular localization analysis of *MbIAA19*. In contrast to the 35S::GFP protein (which was identified in both the cytoplasm and nucleus when released alone in vivo in the leaf epidermal cells of tobacco), the GFP-IAA19 fusion proteins and mCherry protein were primarily located in the nucleus (Figure 5C). The sequences of the *MbIAA19* promoters in WT and *Dwf* mutant were compared to identify any mutation in the promoter region. A single nucleotide change from G to A (-608 bp) was observed in *Dwf*; it was a heterozygous mutation in *Dwf* mutant and seedlings with *Dwf* phenotype. The altered promoter creates a novel cis-acting element [(A/T)GATA(A/G)], a GATA transcription factor binding site. (Figure 5D). Further, GUS activity was analyzed to assess how variation in the alleles affects the activities of the *MbIAA19* promoter. Interestingly, altered promoters in tobacco leaves exhibited markedly reduced levels of GUS protein and GUS activity (Figure 5E,F and Figure S3). These findings suggest that *MbIAA19* is a candidate gene responsible for the *Dwf* mutant phenotype.

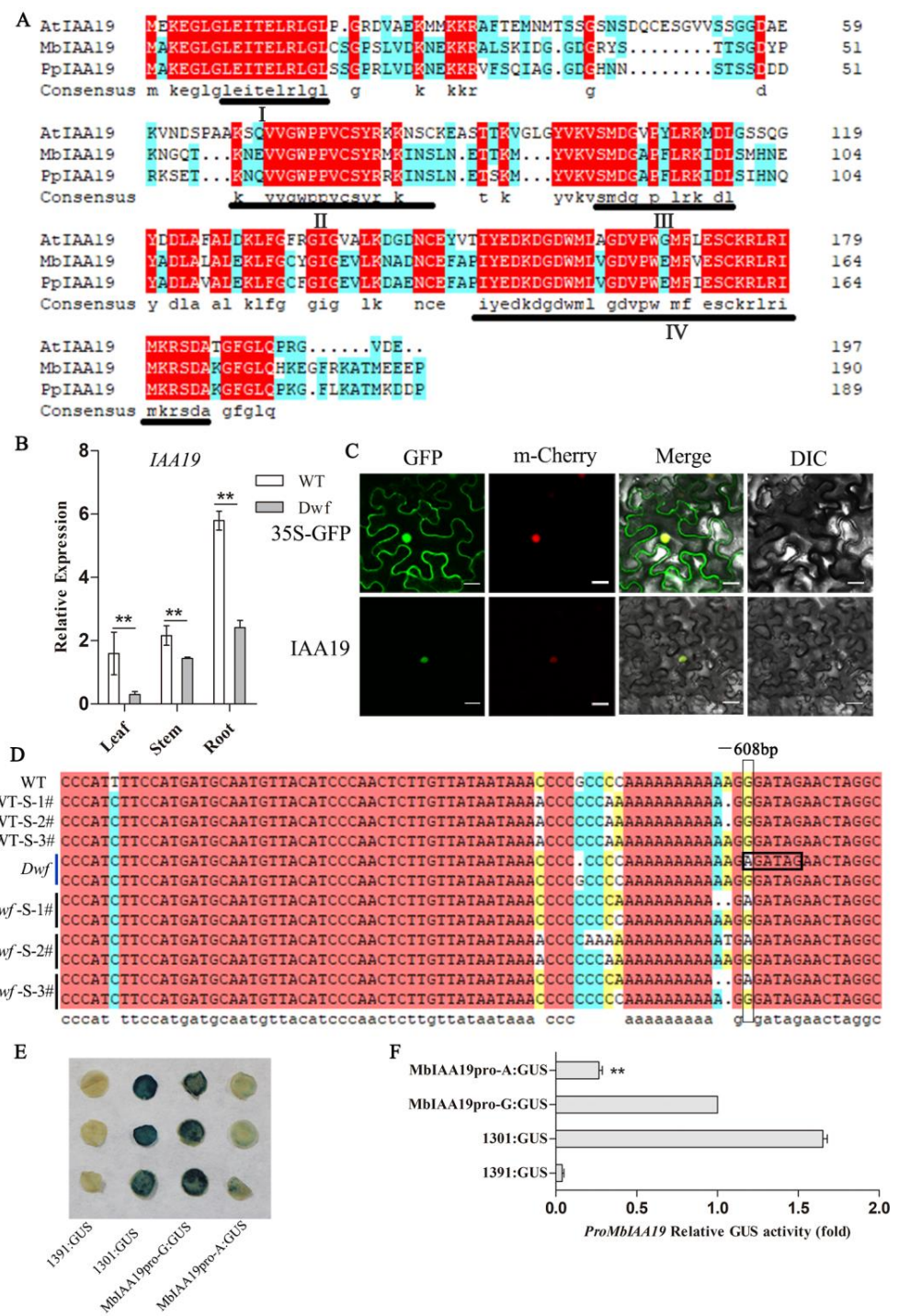


Figure 5. Analysis of *MbIAA19* gene expression and promoter sequence. (A) Amino acid sequence of *MbIAA19* and alignment of *MbIAA19* with *IAA19* protein sequences from *Prunus persica* and *Arabidopsis thaliana*. Four conserved domains (I–IV) of *IAA19* are shown. (B) Relative expression level of *MbIAA19* in different organs of *Dwf* plants compared with WT plants. (C) Subcellular localization analysis of *MbIAA19*. (D) Variations of alleles in the *MbIAA19* promoter between WT, *Dwf*, and seedlings (WT-S1-3# and *Dwf*-S1-3#), the black box represents the novel cis-acting element [(A/T)GATA(A/G)]. (E) The GUS activity of *MbIAA19* promoter in infected tobacco leaves, GUS:1301 and GUS:1391 served as positive and negative controls, respectively. (F) Quantitative assessment of relative GUS activity in infected tobacco leaves. Different colors in (A,D) represent sequences with different levels of conservation. The asterisks above the error bars in (B,F) indicate significant differences at $p < 0.01$ using a one-way analysis of variance (ANOVA) and Dunnett’s test.

2.5. Downregulation of *MbIAA19* Inhibited Plant Height and Internode Length in GL-3

The function of *MbIAA19* and its role in growth regulation in *Malus* was confirmed using GL-3, the open-pollinated cultivar of *M. domestica* 'Royal Gala'. GL-3 was transformed with the vector *RNAi-IAA19*. From all the regenerated lines, five distinct lines with *MbIAA19* downregulation (*RNAi-IAA19*) were obtained. The phenotypes of all five *RNAi-IAA19* plants mimicked the phenotype of *Dwf* mutant, with clearly reduced stature and fewer roots (Figure 6A). For the subsequent studies, two *RNAi-IAA19* lines (8# and 15#) with significant reduction in *MbIAA19* expression were selected (Figure 6B).

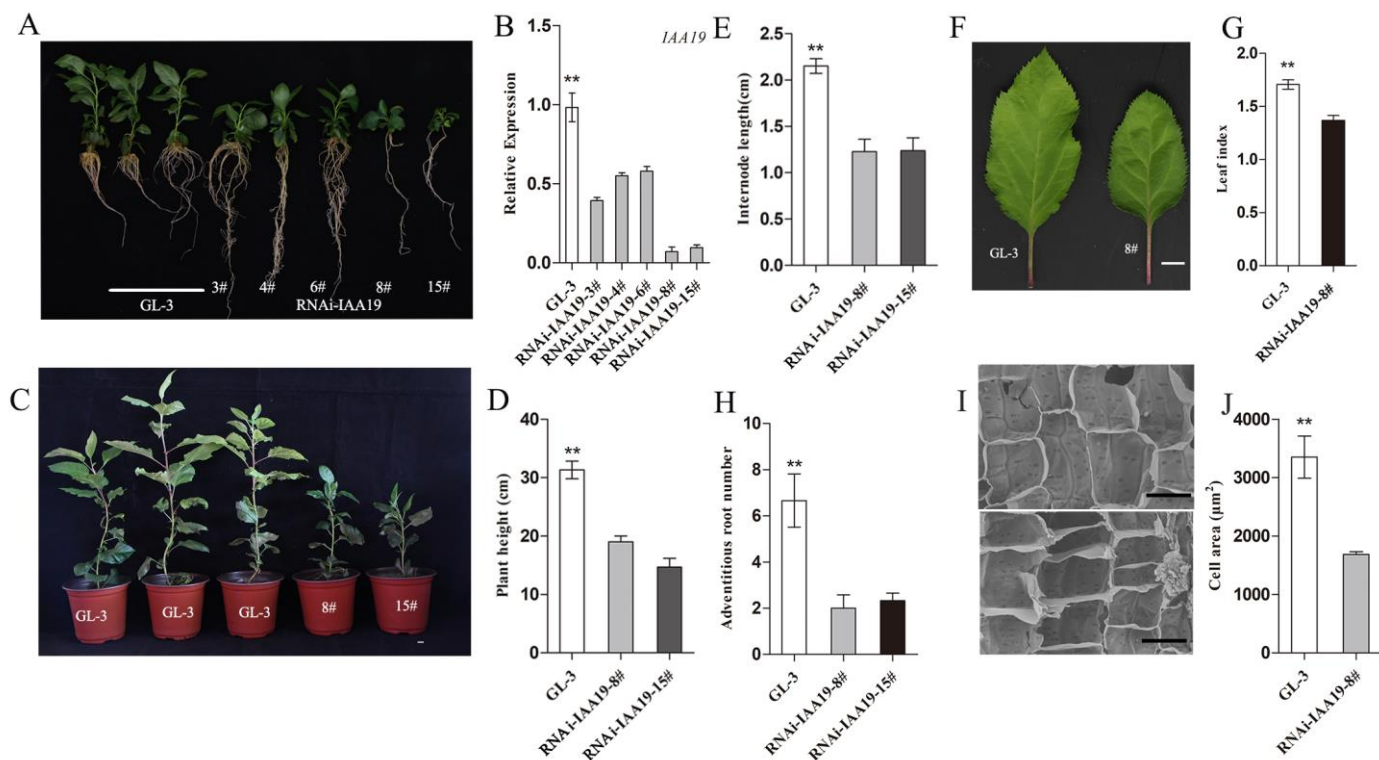


Figure 6. Morphological characterization of the *RNAi-IAA19* lines compared with GL-3. (A) Universal morphology of GL-3 and five *RNAi-IAA19* lines. (B) Expression level of *IAA19* in GL-3 and five *RNAi-IAA19* lines. (C) GL-3 and *RNAi-IAA19* lines after grown in the incubator for 2 months. Scale bar = 1 cm. (D) Plant height of GL-3 and two *RNAi-IAA19* lines (8# and 15#). (E) Internode length of GL-3 and two *RNAi-IAA19* lines (8# and 15#). (F) Images of the leaves from the third leaves of 2-month-old seedlings of GL-3 and *RNAi-IAA19-8#*. Scale bar = 1 cm. (G) Comparison of the ratio of leaf length to width of *RNAi-IAA19* lines and GL-3. (H) Adventitious root numbers of GL-3 and two *RNAi-IAA19* lines (8# and 15#). (I) Scanning electron microscopic analysis of longitudinal segment of the stems of GL-3 (up) and *RNAi-IAA19-8#* (down), Scale bar = 40 µm. (J) Calculation of cell areas of the stems of GL-3 and *RNAi-IAA19-8#*. The asterisks above the error bars in (B,D,E,G,H,J) indicate significant differences at $p < 0.01$ using a one-way ANOVA and Dunnett's test.

After cultivating in a greenhouse for 2 months, compared with GL-3 plants, plant height dramatically reduced by 34% and 49% in the *RNAi-IAA19* lines 8# and 15#, respectively. Their plant height was comparable with that of *Dwf* mutant (Figure 6C,D). The internode length was significantly reduced by approximately 43% in 8# and 15#; the variation in the internode length was wider than that in *Dwf* mutant (Figure 6E). The leaf index was lower than that of GL-3; it was similar to that of *Dwf* mutant, which exhibited shorter leaf length (Figure 6F,G). The *RNAi-IAA19* lines exhibited less adventitious roots (Figure 6H). According to SEM analysis, the cell areas of longitudinal cells were reduced by 54%. The effect of inhibition of cell expansion on dwarf plants was further determined

(Figure 6I,J). Collectively, the results revealed that *MbIAA19* indeed corresponds to the *Dwf* phenotype.

2.6. Endogenous Auxin Levels Were Lower in the Leaves of *RNAi-IAA19-8#* Than in Those of *GL-3*

To investigate whether the endogenous IAA levels were influenced by the expression level of *MbIAA19*, the endogenous IAA levels were assessed in *GL-3* and *RNAi-IAA19-8#* leaves. The endogenous IAA level in *RNAi-IAA19-8#* leaves was substantially lower than that in *GL-3* leaves (Figure 7). This confirmed that the changes in *MbIAA19* expression are highly associated with the *Dwf* phenotype.

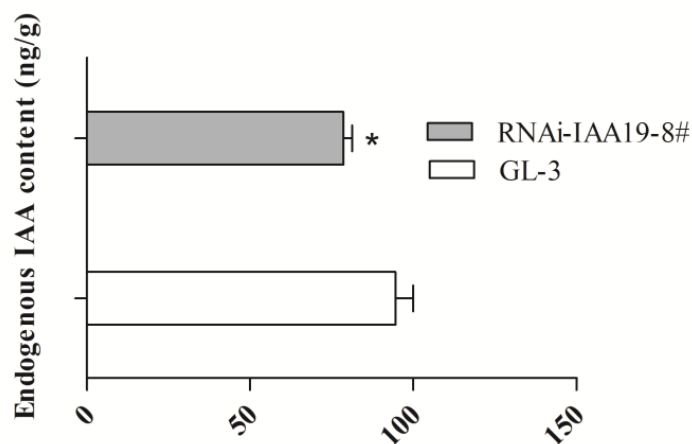


Figure 7. Endogenous auxin levels in *GL-3* and *RNAi-IAA19-8#* leaves. The asterisks above the error bars indicate significant differences at $p < 0.05$ using a one-way ANOVA and Dunnett's test.

3. Discussion

Studies on the development of dwarfing rootstocks and understanding the mechanisms underlying dwarfing are ongoing in apple. Many excellent dwarfing rootstocks have been developed [42]. Numerous dwarf lines of *Malus* have been discovered [10,43,44], and widely accepted standards for evaluating dwarfing rootstocks have been established [38,45]. Additionally, some studies have attempted to explain the mechanism of occurrence of dwarf phenotypes from various perspectives, including the role of phytohormones and nutrient metabolism [46,47]. In this study, the *Dwf* mutant exhibited phenotypic changes in various organs (Figures 1 and 2). From the results, it can be concluded that the inhibition of vessel cell expansion causes the dwarfism in *Dwf* mutant (Figure 1I); however, due to the hypodevelopment of vessels, a potential decrease in nutrient transport capability can also be a cause of dwarfism.

Previous studies have revealed that phytohormones are important factors that regulate dwarfism. Increase in the endogenous or exogenous concentrations of auxin [11,48], gibberellins [49], and brassinosteroid [50] promotes the plant height during suitable levels. The *Dwf* mutant exhibits low concentrations of endogenous IAA (Figure 4A), which is consistent with previous studies [11,48]. RNA-seq revealed several DEGs related to auxin, ET, gibberellin, and brassinolide signaling in *Dwf* mutant (Figure 3A–C). However, no significant DEG related to auxin biosynthesis was identified in *Dwf* mutant (Figure S4). Therefore, the reason underlying the lower endogenous auxin levels should be identified.

As one of major molecular components families (*Aux/IAAs*, *ARFs*, *ABP1* and *TIR1*) involved in auxin signaling, increasing the stability of *Aux/IAA* proteins leads to the disruption or obstruction of auxin signaling, which could even lead to a mutation that was unresponsive to auxin [22,51]. We concluded that the majority of *Aux/IAA* family members have multiple roles in regulating morphogenesis with regard to the development of plant organs. As a result, the *Aux/IAA* gene family may be a suitable candidate and a starting point to understand the mechanism of multi-organ variation during evolution. However, *Aux/IAA* members are rarely studied in the *Malus* species. Previous studies

on Aux/IAA in *Malus* primarily focused on stress resistance, and little attention has been paid to fruit development and plant phenotypes [52–54]. *MbIAA19* was the only major component involved in auxin signaling identified by RNA-seq with a significant difference between WT and *Dwf*, which was uniformly downregulated in different organs of *Dwf* (Figure 5B). Changes in auxin content stimulate our interest in the relationship between auxin accumulation and signaling because numerous studies have demonstrated the essential feedback regulation between auxin accumulation and signaling pathway; auxin affects the activation of signaling components, while Aux/IAA-ARF affect the accumulation of auxin through further regulating the expression of PINs [55,56]. Sequence analyses were used to investigate the sequence changes that may affect gene expression of *IAA19*; fortunately, a single nucleotide change in the promoter of *MbIAA19* resulted in a novel cis-acting element [(A/T)GATA(A/G)], a GATA transcription factor binding site [57,58]. It is tempting to speculate that reduced promoter activity (Figure 5D–F) was because of a transcriptional repressor binding to the novel element. These results prompted us to investigate if *MbIAA19* is involved in determining the dwarfing phenotype in *Dwf* mutant. In this study, *RNAi-IAA19* lines were generated in an attempt to promote the studies on morphological regulation related to the Aux/IAA members in *Malus*.

The inhibition of plant height, internode elongation, and root development by the downregulation of *MbIAA19* was confirmed in two stable *RNAi-IAA19* transgenic lines. This indicated that *MbIAA19* may act across multiple tissues (Figure 6). However, in addition to shorter stems, smaller leaves, and fewer roots, the *Dwf* mutant also exhibits variation in leaf shape, corolla width, and fruit diameter (Figures 1C and 2E–H). It is unclear whether these phenotypes related to the reproductive organs will manifest in the *RNAi-IAA19* lines. Similar to the *Dwf* mutant, low concentrations of endogenous IAA were exhibited in *RNAi-IAA19* lines (Figure 7). This indicated that *MbIAA19* is related to *Dwf* phenotype and has an impact on endogenous auxin content. The known phenotypic variations in *RNAi-IAA19* did not precisely match with those in *Dwf* mutant, e.g., curled leaves were not observed, suggesting that *MbIAA19* may not be the only gene responsible for the variation in *Dwf* mutant phenotype. Therefore, further studies are needed to assess other gene families responsible for the dwarfing mechanism in *Dwf* mutant. Overall, *MbIAA19* regulates the morphology of multiple organs, and the phenotypes of developmental repression are related to the inhibition of *IAA19* expression. Sequence analysis indicated that the closest homolog to *MbIAA19* in *A. thaliana* is *AtIAA19/MSG2*. In *A. thaliana*, *AtIAA19* is involved in the regulation of stamen filament development, plays a key role in the formation of roots, and reveals defects in tropic responses in hypocotyls [59–62]. Indeed, the *RNAi-IAA19* lines and *msg2* mutant exhibited a reduced number of lateral roots (Figure 6I) [61]. The *RNAi-IAA19* lines exhibited significant changes in plant height, internode length, and leaf shape in *Malus* (Figure 6B,E–H), which were not reported in previous studies. Differences in the expression of *MbIAA19* did not cause defective tropic responses, indicating that functional divergence occurred between *Malus* and *A. thaliana*. *PpIAA19* and *VoIAA19* function as growth promoters for plant height; over-expressing *PpIAA19* in tomato (*Solanum lycopersicum* cv. ‘Micro-Tom’) indicated that *PpIAA19* was involved in promoting root length and stem elongation, inhibiting fruit development and fertilization [35]; over-expression of *VoIAA19* in *A. thaliana* also had a notable effect on plant growth, which exhibited higher plant and longer roots than the WT [63]. The above results suggested a new function of *MbIAA19* to modulate *Malus* plants, dwarfing growth.

In conclusion, we identified a differentially expressed transcription factor gene in the *Dwf* mutant. This mutant exhibited lower endogenous IAA level and stable downregulation of *MbIAA19*. A single nucleotide variation in the promoter of *MbIAA19* in *Dwf* resulted in lower promoter activity than that in WT. The downregulation of *MbIAA19* inhibited plant height and internode length. The endogenous IAA levels were lower in *RNAi-IAA19* lines as well, demonstrating the association between *MbIAA19* and the phenotype of *Dwf* mutant. In the future, it will be interesting to clarify how *MbIAA19* is associated with endogenous IAA levels.

4. Materials and Methods

4.1. Plant Material

Dwf mutant, the dwarf mutant of *M. baccata*, was obtained through a natural mutation of *M. baccata* from Hulunbeier League, Inner Mongolia (48.01363 N, 122.73757 E) in China. Previous genetic analyses have suggested that the dwarfing trait of *Dwf* is a quality trait controlled by a dominant heterozygous gene [64]. Therefore, the seedlings of *Dwf* were of two types, dwarf and wild type in 1:1 ratio. Fortunately, the dwarf plants exhibit extremely similar multi-organ linkage variation in the roots, stems, leaves, flowers, and fruits, providing sufficient materials for the successful execution of this study. This study included three WT (WT 1–3) and three *Dwf* plants (*Dwf* 1–3). After vernalization, the seeds collected from *Dwf* plants were sown in soil. The plants were grown in a smart incubator at 25 °C with 12 h:12 h (light: dark cycle) and 70% relative humidity. To establish in vitro shoot proliferation in GL-3 (the open-pollinated cultivar of *M. domestica* 'Royal Gala'), MS media containing 3% sucrose and 0.7% agar (*w/v*) supplemented with 0.3 mg L⁻¹ 6-benylaminopurine (6-BA), 0.2 mg L⁻¹ indole acetic acid (IAA), and 0.1 mg L⁻¹ gibberellic acid (GA3) were used.

4.2. Phenotypic and Cytological Analyses

The botanical traits investigated in this study included plant height, internode length, leaf index, primary roots length, primary lateral root number, corolla width, and fruit diameter. The leaf index was calculated as the leaf length to width ratio. One-month-old seedlings were used to measure plant height, whereas two-month-old seedlings were used to measure the changes in plant height after IAA treatment. The primary root length was measured using 1-week-old seedlings. The internode lengths were analyzed using the annual branches of WT and *Dwf* plants. The leaf length and width, root length, fruit diameter, and corolla were measured using a vernier caliper. At least three biological replicates were used for the analysis, and the average of each index was calculated.

Scanning electron microscopy (SEM; HITACHI Regulus 8100, Hitachi, Tokyo, Japan) was performed to study the stems of WT and *Dwf* plants. The third internode of annual branches was prepared as follows. The internodes were rinsed three times with PBS after fixing in 2.5% glutaraldehyde. Further, the samples were dehydrated using ethanol gradients and substituted with tertiary butyl alcohol. After they were dried (VFD-30) and sprayed with gold (MC1000), the images were acquired using SEM. ImageJ2 software (NIH, Bethesda, MD, USA) was used to measure the cellular areas in the longitudinal section of vessels of stem.

4.3. RNA-seq Analysis and Gene Expression

Total RNA was extracted from the young leaves of WT 1–3 and *Dwf* mutant 1–3. RNA sequencing libraries were constructed and sequenced on an Illumina NovaSeq 6000 system (Illumina, San Diego, CA, USA). RNA-seq data from the two genotypes were analyzed according to the Apple Genome (GDDH13 Version 1.1, <https://iris.angers.inra.fr/gddh13/the-apple-genome-downloads.html>, accessed on 5 June 2017). Quality control and trimming processes were performed as previously described [65]. Fragments per kilobase of transcript per million mapped read (FPKM) values were estimated to analyze the differentially expressed genes (DEGs) between the two genotypes. The genes were considered to be significantly expressed if the absolute fold change was ≥ 1 and *p* was < 0.01 as determined by an R package (R Foundation for Statistical Computing, Vienna, Austria). Gene Ontology (GO, <http://geneontology.org/>, accessed on 1 May 2019) and Kyoto Encyclopedia of Genes and Genomes (KEGG, <http://www.kegg.jp/kegg>, accessed on 1 May 2019) pathway enrichment analyses were performed to annotate the DEGs. All raw and processed RNA-seq data from this study have been released on SRA Run Selector, with the SRA accession number PRJNA543379 (NCBI BioProject, <https://www.ncbi.nlm.nih.gov/Traces/study/?acc=PRJNA543379>, accessed on 15 June 2020).

Total RNA of leaves extraction was conducted using CTAB as described previously [66]. The cDNA was generated using PrimeScript™ RT reagent Kit with gDNA Eraser (TaKaRa, Dalian, China). The TB Green® Premix Ex Taq™II (TaKaRa) and ABI QuantStudio 6 Flex instrument (Applied Biosystems, Waltham, MA, USA) were used for quantitative PCR (qPCR) analyses. Reaction system and qPCR process were conducted as described previously [66]. RNA extracted from each plant was used as one biological replicate, and a total of three technical and biological replicates to calculate the variances of population (SD). The expression levels were standardized with those of the *18S* genes. Specific primers are listed in Supporting Information (Table S1).

4.4. Determination of the Contents of Endogenous IAA

The contents of endogenous IAA were determined as previously described [67] using 0.5 g young leaves of WT and *Dwf* mutant plants. The experiment involved three biological and technical replicates. [¹³C]₆-IAA (OlChemIm Company, Olomouc, Czech Republic) was used as the internal standard.

4.5. Exogenous IAA Treatment

One-month-old seedlings with *Dwf* phenotype were sprayed with 0.4 mg·L⁻¹ IAA once a week for 4 weeks, spraying with water as control. The experiment was performed in three biological replicates.

4.6. Cloning, Plasmid Construction, and Genetic Transformation

The full-length sequence of the promoter and sense strand of *MbIAA19* (MD17G1198100) was searched in the genomics database for the Rosaceae family (GDR, <https://www.rosaceae.org/>, accessed on 7 August 2017). The full length 1600-bp promoter sequence of WT and *Dwf* mutant plants was cloned into the binary vector pCambia1391 for sequencing and GUS activity analysis. The CDSs were subcloned from the leaves of *Dwf* mutant plants into 35S::GFP to create 35S::IAA19:GFP, and antisense partial sequences were amplified to create antisense suppression vectors (*RNAi::IAA19*). Vectors were constructed using ClonExpress II One Step Cloning Kit (C115, Vazyme, Nanjing, China). The primers are listed in Supporting Information (Table S1).

4.7. Confocal Microscopy and GFP and GUS Analyses

Constructed vectors were introduced into *Agrobacterium tumefaciens* GV3101, which was used to infect the leaves of 4-week-old tobacco (*Nicotina benthamiana*) plants. Green fluorescent protein (GFP) and red fluorescent protein (mCherry) were observed using a laser scanning confocal microscope (TCS SP8, Leica, Wetzlar, Germany). The excited points of GFP and mCherry were selected as previously [68]. For detecting GUS activity in the infected tobacco leaves, GUS staining was performed. The infected leaves were incubated with X-Gluc buffer for 48 h at 37 °C and soaked in ethanol to remove chlorophyll. Further, fluorometric assays were performed for assessing GUS activity as previously described [69].

4.8. Plant Transformation

The *RNAi::IAA19* vector was introduced into the *A. tumefaciens* strain EHA105. The young leaves of in vitro-grown “GL-3” were used for transformation. The transformed bacterial cells were incubated in LB medium at 28 °C, 180 rpm for 12–15 h, then diluted to OD₆₀₀ = 0.5 in MS medium containing 1.5% sucrose and 0.5% glucose (*w/v*) supplemented with 100 μM acetosyringone (AS). The young leaves were cut into segments 3 mm wide, then the segments were gently shaken in bacterial suspension for 8 min. After transformation, the segments were transferred into co-culture medium for 3 d in the dark. Then the segments were cultivated on a selective medium containing 50 mg·L⁻¹ kanamycin (Kan), 250 mg·L⁻¹ cefixime (Cef) and 250 mg·L⁻¹ timentin (Tim) for a few months, which were changed every half a month. The incubation was in the conditions of room temperature

25 °C and a photoperiod of 16 h:8 h (light:dark). Finally, mediums were configured as described by Dai et al. [70].

4.9. Statistical Analysis

The significant differences in the phenotypic data, gene expression, IAA production, and GUS activity were assessed using one-way analysis of variance (ANOVA) and Dunnett's test (** $p < 0.01$, * $p < 0.05$) as specified in the figure legends. Each sample was evaluated at least three times.

Supplementary Materials: The following supporting information can be downloaded at: <https://www.mdpi.com/article/10.3390/plants12173097/s1>, Figure S1: DEGs between the WT and *Dwf* mutant; Figure S2: Confirmation of the DEGs by quantitative real time-PCR (qRT-PCR); Figure S3: The GUS activity of MbIAA19 promoter in tobacco leaves. Figure S4: A heat map of seven TAR genes (tryptophan aminotransferase-related gene) and nine YUCCA genes (indole-3-pyruvate monooxygenase gene) in the WT and *Dwf* identified using RNA-seq. Table S1: Primers used in this study.

Author Contributions: Conceptualization, J.W. and W.D.; methodology, X.Z. and Y.H.; software, X.Z.; validation, J.W.; formal analysis, J.W. and D.F.; investigation, J.W.; resources, W.D.; data curation, J.W. and L.X.; writing—original draft preparation, J.W.; writing—review and editing, J.W. and L.X.; visualization, J.W. and K.Z.; supervision, W.D.; project administration, W.D.; funding acquisition, W.D. All authors have read and agreed to the published version of the manuscript.

Funding: This work was funded by the project of National Infrastructure of Crop Germplasm Resources—Sub infrastructure of Hawthorn, China: [NICGR-2019-057].

Data Availability Statement: All the raw and operated RNA-seq data applied in this work have been released on SRA Run Selector, with the SRA accession number PRJNA543379 (NCBI BioProject, <https://www.ncbi.nlm.nih.gov/Traces/study/?acc=PRJNA543379>, accessed on 15 June 2020).

Acknowledgments: We appreciate the GL-3 material provided by Zhihong Zhang and Hongyan Dai (Shenyang Agriculture University) for the transformation experiment.

Conflicts of Interest: The authors declare no conflict of interest.

References

- Gregory, P.J.; George, T.S. Feeding nine billion: The challenge to sustainable crop production. *J. Exp. Bot.* **2011**, *62*, 5233–5239. [[CrossRef](#)]
- Opio, P.; Tomiyama, H.; Saito, T.; Ohkawa, K.; Ohara, H.; Kondo, S. Paclobutrazol elevates auxin and abscisic acid, reduces gibberellins and zeatin and modulates their transporter genes in *Marubakaido* apple (*Malus prunifolia* Borkh. var. ringo Asami) rootstocks. *Plant Physiol. Biochem.* **2020**, *155*, 502–511. [[CrossRef](#)] [[PubMed](#)]
- Zheng, X.; Zhang, H.; Xiao, Y.; Wang, C.; Tian, Y. Deletion in the Promoter of *PcPIN-L* Affects the Polar Auxin Transport in Dwarf Pear (*Pyrus communis* L.). *Sci. Rep.* **2019**, *9*, 18645. [[CrossRef](#)] [[PubMed](#)]
- Mori, M.; Nomura, T.; Ooka, H.; Ishizaka, M.; Yokota, T.; Sugimoto, K.; Okabe, K.; Kajiwara, H.; Satoh, K.; Yamamoto, K.; et al. Isolation and characterization of a rice dwarf mutant with a defect in brassinosteroid biosynthesis. *Plant Physiol.* **2022**, *130*, 1152–1161. [[CrossRef](#)] [[PubMed](#)]
- Zhang, X.; He, L.; Zhao, B.; Zhou, S.; Li, Y.; He, H.; Bai, Q.; Zhao, W.; Guo, S.; Liu, Y.; et al. Dwarf and Increased Branching 1 controls plant height and axillary bud outgrowth in *Medicago truncatula*. *J. Exp. Bot.* **2020**, *71*, 6355–6365. [[CrossRef](#)]
- Lan, J.; Lin, Q.; Zhou, C.; Ren, Y.; Liu, X.; Miao, R.; Jing, R.; Mou, C.; Nguyen, T.; Zhu, X.; et al. Small grain and semi-dwarf 3, a WRKY transcription factor, negatively regulates plant height and grain size by stabilizing *SLR1* expression in rice. *Plant Mol. Biol.* **2020**, *104*, 429–450. [[CrossRef](#)]
- Hirano, K.; Yoshida, H.; Aya, K.; Kawamura, M.; Hayashi, M.; Hobo, T.; Sato-Izawa, K.; Kitano, H.; Ueguchi-Tanaka, M.; Matsuoka, M. SMALL ORGAN SIZE 1 and SMALL ORGAN SIZE 2/DWARF AND LOW-TILLERING form a complex to integrate auxin and brassinosteroid signaling in rice. *Mol. Plant* **2017**, *10*, 590–604. [[CrossRef](#)]
- Chen, T.; Xiao, W.; Huang, C.; Zhou, D.; Liu, Y.; Guo, T.; Chen, Z.; Wang, H. Fine Mapping of the Affecting Tillering and Plant Height Gene *CHA-1* in Rice. *Plants* **2023**, *12*, 1507. [[CrossRef](#)]
- Li, H.; Wang, L.; Liu, M.; Dong, Z.; Li, Q.; Fei, S.; Xiang, H.; Liu, B.; Jin, W. Maize plant architecture is regulated by the ethylene biosynthetic gene *ZmACS7*. *Plant Physiol.* **2020**, *183*, 1184–1199. [[CrossRef](#)]
- Wang, L.; Guo, J.; Chu, Y.; Pan, Q.; Zhu, Y. MdCo31 interacts with an RNA polymerase II transcription subunit 32 to regulate dwarf growth with short internodes in columnar apple. *Plant Sci.* **2022**, *325*, 111496. [[CrossRef](#)]

11. Bai, Y.; Cai, M.; Mu, C.; Zheng, H.; Cheng, Z.; Xie, Y.; Gao, J. Integrative analysis of exogenous auxin mediated plant height regulation in Moso bamboo (*Phyllostachys edulis*). *Ind. Crop. Prod.* **2023**, *200*, 116852. [[CrossRef](#)]
12. Gamuyao, R.; Nagai, K.; Ayano, M.; Mori, Y.; Minami, A.; Kojima, M.; Suzuki, T.; Sakakibara, H.; Higashiyama, T.; Ashikari, M.; et al. Hormone distribution and transcriptome profiles in bamboo shoots provide insights on bamboo stem emergence and growth. *Plant Cell Physiol.* **2017**, *58*, 702–716. [[CrossRef](#)]
13. Hu, D.G.; Wang, N.; Wang, D.H.; Cheng, L.; Wang, Y.X.; Zhao, Y.W.; Ding, J.Y.; Gu, K.D.; Xiao, X.; Hao, Y.J. A basic/helix–loop–helix transcription factor controls leaf shape by regulating auxin signaling in apple. *New Phytol.* **2020**, *228*, 1897–1913. [[CrossRef](#)] [[PubMed](#)]
14. Stepanova, A.N.; Robertson-Hoyt, J.; Yun, J.; Benavente, L.M.; Xie, D.Y.; Doležal, K.; Schlereth, A.; Jürgens, G.; Alonso, J.M. TAA1-mediated auxin biosynthesis is essential for hormone crosstalk and plant development. *Cell* **2008**, *133*, 177–191. [[CrossRef](#)] [[PubMed](#)]
15. Li, Z.; Zhang, X.; Zhao, Y.; Li, Y.; Zhang, G.; Peng, Z.; Zhang, J. Enhancing auxin accumulation in maize root tips improves root growth and dwarfs plant height. *Plant Biotechnol. J.* **2018**, *16*, 86–99. [[CrossRef](#)]
16. Habets, M.E.; Offringa, R. PIN-driven polar auxin transport in plant developmental plasticity: A key target for environmental and endogenous signals. *New Phytol.* **2014**, *203*, 362–377. [[CrossRef](#)]
17. Weijers, D.; Wagner, D. Transcriptional responses to the auxin hormone. *Annu. Rev. Plant Biol.* **2016**, *67*, 539–574. [[CrossRef](#)]
18. Jing, H.; Yang, X.; Zhang, J.; Liu, X.; Zheng, H.; Dong, G.; Nian, J.; Feng, J.; Xia, B.; Qian, Q.; et al. Peptidyl-prolyl isomerization targets rice Aux/IAAs for proteasomal degradation during auxin signalling. *Nat. Commun.* **2015**, *6*, 7395. [[CrossRef](#)]
19. Gray, W.M.; Kepinski, S.; Rouse, D.; Leyser, O.; Estelle, M. Auxin regulates SCFTIR1-dependent degradation of AUX/IAA proteins. *Nature* **2001**, *414*, 271–276. [[CrossRef](#)]
20. Hu, J.; Su, H.; Cao, H.; Wei, H.; Fu, X.; Jiang, X.; Song, Q.; He, X.; Xu, C.; Luo, K. AUXIN RESPONSE FACTOR7 integrates gibberellin and auxin signaling via interactions between DELLA and AUX/IAA proteins to regulate cambial activity in poplar. *Plant Cell* **2022**, *34*, 2688–2707. [[CrossRef](#)]
21. Dreher, K.A.; Brown, J.; Saw, R.E.; Callis, J. The Arabidopsis Aux/IAA protein family has diversified in degradation and auxin responsiveness. *Plant Cell* **2006**, *18*, 699–714. [[CrossRef](#)] [[PubMed](#)]
22. Ramos, J.A.; Zenser, N.; Leyser, O.; Callis, J. Rapid degradation of auxin/indoleacetic acid proteins requires conserved amino acids of domain II and is proteasome dependent. *Plant Cell* **2001**, *13*, 2349–2360. [[CrossRef](#)] [[PubMed](#)]
23. Kim, B.C.; Soh, M.C.; Kang, B.J.; Furuya, M.; Nam, H.G. Two dominant photomorphogenic mutations of *Arabidopsis thaliana* identified as suppressor mutations of *hy2*. *Plant J.* **1996**, *9*, 441–456. [[CrossRef](#)] [[PubMed](#)]
24. Nagpal, P.; Walker, L.M.; Young, J.C.; Sonawala, A.; Timpote, C.; Estelle, M.; Reed, J.W. AXR2 encodes a member of the Aux/IAA protein family. *Plant Physiol.* **2000**, *123*, 563–574. [[CrossRef](#)]
25. Rogg, L.E.; Lasswell, J.; Bartel, B. A gain-of-function mutation in IAA28 suppresses lateral root development. *Plant Cell* **2001**, *13*, 465–480. [[CrossRef](#)]
26. Uehara, T.; Okushima, Y.; Mimura, T.; Tasaka, M.; Fukaki, H. Domain II mutations in CRANE/IAA18 suppress lateral root formation and affect shoot development in *Arabidopsis thaliana*. *Plant Cell Physiol.* **2008**, *49*, 1025–1038. [[CrossRef](#)]
27. Park, J.Y.; Kim, H.J.; Kim, J. Mutation in domain II of IAA1 confers diverse auxin-related phenotypes and represses auxin-activated expression of Aux/IAA genes in steroid regulator-inducible system. *Plant J.* **2002**, *32*, 669–683. [[CrossRef](#)]
28. Song, Y.L. The gene *OslAA9* encoding auxin/indole-3-acetic acid proteins is a negative regulator of auxin-regulated root growth in rice. *Biol. Plant* **2019**, *63*, 210–218. [[CrossRef](#)]
29. Deng, W.; Yang, Y.; Ren, Z.; Audran-Delalande, C.; Mila, I.; Wang, X.; Song, H.; Hu, Y.; Bouzayen, M.; Li, Z. The tomato *SllAA15* is involved in trichome formation and axillary shoot development. *New Phytol.* **2012**, *194*, 379–390. [[CrossRef](#)]
30. Wang, H.; Jones, B.; Li, Z.; Frasse, P.; Delalande, C.; Regad, F.; Chaabouni, S.; Latché, A.; Pech, J.C.; Bouzayen, M. The tomato Aux/IAA transcription factor IAA9 is involved in fruit development and leaf morphogenesis. *Plant Cell* **2005**, *17*, 2676–2692. [[CrossRef](#)]
31. Wei, T.; Zhang, L.; Zhu, R.; Jiang, X.; Yue, C.; Su, Y.; Ren, H.; Wang, M. A Gain-of-function mutant of IAA7 inhibits stem elongation by transcriptional repression of *EXPA5* genes in *Brassica napus*. *Int. J. Mol. Sci.* **2021**, *22*, 9018. [[CrossRef](#)] [[PubMed](#)]
32. Xu, C.; Shen, Y.; He, F.; Fu, X.; Yu, H.; Lu, W.; Li, Y.; Li, C.; Fan, D.; Wang, H.C.; et al. Auxin-mediated Aux/IAA-ARF-HB signaling cascade regulates secondary xylem development in *Populus*. *New Phytol.* **2019**, *222*, 752–767. [[CrossRef](#)] [[PubMed](#)]
33. Fu, L.I.; Dong, Y.A.N.; Gao, L.F.; Pan, L.I.U.; Zhao, G.Y.; Jia, J.Z.; Ren, Z.L. *TaIAA15* genes regulate plant architecture in wheat. *J. Integr. Agric.* **2022**, *21*, 1243–1252. [[CrossRef](#)]
34. Bu, H.; Sun, X.; Yue, P.; Qiao, J.; Sun, J.; Wang, A.; Yuan, H.; Yu, W. The *MdAux/IAA2* Transcription Repressor Regulates Cell and Fruit Size in Apple Fruit. *Int. J. Mol. Sci.* **2022**, *23*, 9454. [[CrossRef](#)]
35. Ding, Y.; Zeng, W.; Wang, X.; Wang, Y.; Niu, L.; Pan, L.; Lu, Z.; Gui, G.; Li, G. Over-expression of peach *PpIAA19* in tomato alters plant growth, Parthenocarpy, and fruit shape. *J. Plant Growth Regul.* **2019**, *38*, 103–112. [[CrossRef](#)]
36. Jiang, M.; Hu, H.; Kai, J.; Traw, M.B.; Yang, S.; Zhang, X. Different knockout genotypes of *OsIAA23* in rice using CRISPR/Cas9 generating different phenotypes. *Plant Mol. Biol.* **2019**, *100*, 467–479. [[CrossRef](#)]
37. Norelli, J.L.; Holleran, H.T.; Johnson, W.C.; Robinson, T.L.; Aldwinckle, H.S. Resistance of Geneva and other apple rootstocks to *Erwinia amylovora*. *Plant Dis.* **2003**, *87*, 26–32. [[CrossRef](#)]

38. Harrison, N.; Harrison, R.J.; Barber-Perez, N.; Cascant-Lopez, E.; Cobo-Medina, M.; Lipska, M.; Conde-Ruiz, R.; Brain, P.; Gregory, P.J.; Fernández-Fernández, F. A new three-locus model for rootstock-induced dwarfing in apple revealed by genetic mapping of root bark percentage. *J. Exp. Bot.* **2016**, *67*, 1871–1881. [[CrossRef](#)]
39. Hou, K.; Wu, W.; Gan, S.S. SAUR36, a small auxin up RNA gene, is involved in the promotion of leaf senescence in *Arabidopsis*. *Plant Physiol.* **2013**, *161*, 1002–1009. [[CrossRef](#)]
40. Potuschak, T.; Lechner, E.; Parmentier, Y.; Yanagisawa, S.; Grava, S.; Koncz, C.; Genschik, P. EIN3-dependent regulation of plant ethylene hormone signaling by two *Arabidopsis* F box proteins: EBF1 and EBF2. *Cell* **2003**, *115*, 679–689. [[CrossRef](#)]
41. Major, I.T.; Guo, Q.; Zhai, J.; Kapali, G.; Kramer, D.M.; Howe, G.A. A Phytochrome B-Independent Pathway Restricts Growth at High Levels of Jasmonate Defense. *Plant Physiol.* **2020**, *183*, 733–749. [[CrossRef](#)] [[PubMed](#)]
42. Wang, Y.; Li, W.; Xu, X.; Qiu, C.; Wu, T.; Wei, Q.; Ma, F.; Han, Z. Progress of apple rootstock breeding and its use. *Hortic. Plant J.* **2019**, *5*, 183–191. [[CrossRef](#)]
43. Jindal, K.K.; Dalbro, S.; Andersen, A.S.; Poll, L. Endogenous growth substances in normal and dwarf mutants of Cortland and Golden Delicious apple shoots. *Physiol. Plant.* **1974**, *32*, 71–77. [[CrossRef](#)]
44. Looney, N.E.; Lane, W.D. Spur-type growth mutants of McIntosh apple: A review of their genetics, physiology and field performance. In *International Workshop on Controlling Vigor in Fruit Trees*; International Society for Horticultural Science (ISHS): Leuven, Belgium, 1983; Volume 146, pp. 31–46. [[CrossRef](#)]
45. Wang, S.Y.; Faust, M. The relationship of internode length to carbohydrate content in genetic dwarf apple trees. *Sci. Hortic.* **1987**, *33*, 197–203. [[CrossRef](#)]
46. Soumelidou, K.; Morris, D.A.; Battey, N.H.; Barnett, J.R.; John, P. Auxin transport capacity in relation to the dwarfing effect of apple rootstocks. *J. Hortic. Sci.* **1994**, *69*, 719–725. [[CrossRef](#)]
47. Li, S.; Zhang, Y.; Chen, H.; Li, B.; Liang, B.; Xu, J. The Effect of Dwarfing Interstocks on Vegetative Growth, Fruit Quality and Ionome Nutrition of ‘Fuji’ Apple Cultivar ‘Tianhong 2’—A One-Year Study. *Plants* **2023**, *12*, 2158. [[CrossRef](#)]
48. Guo, F.; Huang, Y.; Qi, P.; Lian, G.; Hu, X.; Han, N.; Wang, J.; Zhu, M.; Qian, Q.; Bian, H. Functional analysis of auxin receptor OsTIR1/OsAFB family members in rice grain yield, tillering, plant height, root system, germination, and auxinic herbicide resistance. *New Phytol.* **2021**, *229*, 2676–2692. [[CrossRef](#)]
49. Sasaki, A.; Ashikari, M.; Ueguchi-Tanaka, M.; Itoh, H.; Nishimura, A.; Swapan, D.; Ishiyama, K.; Saito, T.; Kobayashi, M.; Khush, G.S.; et al. A mutant gibberellin-synthesis gene in rice. *Nature* **2022**, *416*, 701–702. [[CrossRef](#)]
50. Hu, S.; Wang, C.; Sanchez, D.L.; Lipka, A.E.; Liu, P.; Yin, Y.; Blanco, M.; Lübberstedt, T. Gibberellins promote brassinosteroids action and both increase heterosis for plant height in maize (*Zea mays* L.). *Front. Plant Sci.* **2017**, *8*, 1039. [[CrossRef](#)]
51. Lv, B.; Yu, Q.; Liu, J.; Wen, X.; Yan, Z.; Hu, K.; Li, H.; Kong, X.; Li, C.; Tian, H.; et al. Non-canonical AUX/IAA protein IAA 33 competes with canonical AUX/IAA repressor IAA 5 to negatively regulate auxin signaling. *EMBO J.* **2020**, *39*, e101515. [[CrossRef](#)] [[PubMed](#)]
52. Wang, L.; Xu, K.; Li, Y.; Cai, W.; Zhao, Y.; Yu, B.; Zhu, Y. Genome-wide identification of the Aux/IAA family genes (*MdIAA*) and functional analysis of *MdIAA18* for apple tree ideotype. *Biochem. Genet.* **2019**, *57*, 709–733. [[CrossRef](#)] [[PubMed](#)]
53. Huang, D.; Wang, Q.; Jing, G.; Ma, M.; Li, C.; Ma, F. Overexpression of *MdIAA24* improves apple drought resistance by positively regulating strigolactone biosynthesis and mycorrhization. *Tree Physiol.* **2021**, *41*, 134–146. [[CrossRef](#)]
54. Huang, D.; Wang, Q.; Duan, D.; Dong, Q.; Zhao, S.; Zhang, M.; Jing, G.; Liu, C.; van Nocker, S.; Ma, F.; et al. Overexpression of *MdIAA9* confers high tolerance to osmotic stress in transgenic tobacco. *Peer J.* **2019**, *7*, e7935. [[CrossRef](#)] [[PubMed](#)]
55. Chen, Q.; Liu, Y.; Maere, S.; Lee, E.; Van Isterdael, G.; Xie, Z.; Xuan, W.; Lucas, J.; Vassileva, V.; Kitakura, S.; et al. A coherent transcriptional feed-forward motif model for mediating auxin-sensitive *PIN3* expression during lateral root development. *Nat. Commun.* **2015**, *6*, 8821. [[CrossRef](#)]
56. Krogan, N.T.; Marcos, D.; Weiner, A.I.; Berleth, T. The auxin response factor MONOPTEROS controls meristem function and organogenesis in both the shoot and root through the direct regulation of *PIN* genes. *New Phytol.* **2016**, *212*, 42–50. [[CrossRef](#)]
57. Zhang, C.; Huang, Y.; Xiao, Z.; Yang, H.; Hao, Q.; Yuan, S.; Chen, H.; Chen, L.; Chen, S.; Zhou, X.; et al. A GATA Transcription Factor from Soybean (*Glycine max*) Regulates Chlorophyll Biosynthesis and Suppresses Growth in the Transgenic *Arabidopsis thaliana*. *Plants* **2020**, *9*, 1036. [[CrossRef](#)]
58. Bi, Y.M.; Zhang, Y.; Signorelli, T.; Zhao, R.; Zhu, T.; Rothstein, S. Genetic analysis of *Arabidopsis* GATA transcription factor gene family reveals a nitrate-inducible member important for chlorophyll synthesis and glucose sensitivity. *Plant J.* **2005**, *44*, 680–692. [[CrossRef](#)]
59. Zhou, X.Y.; Song, L.; Xue, H.W. Brassinosteroids regulate the differential growth of *Arabidopsis* hypocotyls through auxin signaling components IAA19 and ARF7. *Mol. Plant* **2013**, *6*, 887–904. [[CrossRef](#)] [[PubMed](#)]
60. Tashiro, S.; Tian, C.E.; Watahiki, M.K.; Yamamoto, K.T. Changes in growth kinetics of stamen filaments cause inefficient pollination in *massugu2*, an auxin insensitive, dominant mutant of *Arabidopsis thaliana*. *Physiol. Plant* **2009**, *137*, 175–187. [[CrossRef](#)]
61. Muto, H.; Watahiki, M.K.; Nakamoto, D.; Kinjo, M.; Yamamoto, K.T. Specificity and similarity of functions of the *Aux/IAA* genes in auxin signaling of *Arabidopsis* revealed by promoter-exchange experiments among *MSG2/IAA19*, *AXR2/IAA7*, and *SLR/IAA14*. *Plant Physiol.* **2007**, *144*, 187–196. [[CrossRef](#)]
62. Tatematsu, K.; Kumagai, S.; Muto, H.; Sato, A.; Watahiki, M.K.; Harper, R.M.; Liscum, E.; Yamamoto, K.T. *MASSUGU2* encodes Aux/IAA19, an auxin-regulated protein that functions together with the transcriptional activator NPH4/ARF7 to regulate differential growth responses of hypocotyl and formation of lateral roots in *Arabidopsis thaliana*. *Plant Cell* **2004**, *16*, 379–393. [[CrossRef](#)] [[PubMed](#)]

63. Kohno, M.; Takato, H.; Horiuchi, H.; Fujita, K.; Suzuki, S. Auxin-nonresponsive grape *Aux/IAA19* is a positive regulator of plant growth. *Mol. Biol. Rep.* **2012**, *39*, 911–917. [[CrossRef](#)] [[PubMed](#)]
64. Meng, Q. Discovery of extremely cold-resistant dwarf germplasm resources in the genus Apple. *Chin. Fruit Trees* **1991**, *3*, 42. [[CrossRef](#)]
65. Liu, J.; Wang, J.; Wang, M.; Zhao, J.; Zheng, Y.; Zhang, T.; Xue, L.; Lei, J. Genome-wide analysis of the *R2R3-MYB* gene family in *Fragaria × ananassa* and its function identification during anthocyanins biosynthesis in Pink-flowered Strawberry. *Front. Plant Sci.* **2021**, *12*, 702160. [[CrossRef](#)] [[PubMed](#)]
66. Li, T.; Tan, D.; Liu, Z.; Jiang, Z.; Wei, Y.; Zhang, L.; Li, X.; Yuan, H.; Wang, A. Apple *MdACS6* Regulates Ethylene Biosynthesis during Fruit Development Involving Ethylene-Responsive Factor. *Plant Cell Physiol.* **2015**, *56*, 1909–1917. [[CrossRef](#)] [[PubMed](#)]
67. Bu, H.; Yu, W.; Yuan, H.; Yue, P.; Wei, Y.; Wang, A. Endogenous auxin content contributes to larger size of apple fruit. *Front. Plant Sci.* **2020**, *11*, 592540. [[CrossRef](#)]
68. Zhang, S.; Feng, M.; Chen, W.; Zhou, X.; Lu, J.; Wang, Y.; Li, Y.; Jiang, C.Z.; Gan, S.S.; Ma, N.; et al. In rose, transcription factor PTM balances growth and drought survival via PIP2; 1 aquaporin. *Nat. Plants* **2019**, *5*, 290–299. [[CrossRef](#)]
69. Wang, C.; Gao, G.; Cao, S.; Xie, Q.; Qi, H. Isolation and functional validation of the *CmLOX08* promoter associated with signalling molecule and abiotic stress responses in oriental melon, *Cucumis melo* var. *makuwa* Makino. *BMC Plant Biol.* **2019**, *19*, 75. [[CrossRef](#)]
70. Dai, H.; Li, W.; Han, G.; Yang, Y.I.; Ma, Y.; Li, H.E.; Zhang, Z. Development of a seedling clone with high regeneration capacity and susceptibility to *Agrobacterium* in apple. *Sci. Hort.* **2013**, *164*, 202–208. [[CrossRef](#)]

Disclaimer/Publisher’s Note: The statements, opinions and data contained in all publications are solely those of the individual author(s) and contributor(s) and not of MDPI and/or the editor(s). MDPI and/or the editor(s) disclaim responsibility for any injury to people or property resulting from any ideas, methods, instructions or products referred to in the content.